The anti-inflammatory effects of agmatine on transient focal cerebral ischemia in diabetic rats

Jeong Min Kim
Department of Medicine

The Graduate School, Yonsei University

The anti-inflammatory effects of agmatine on transient focal cerebral ischemia in diabetic rats

Directed by Professor Bon-Nyeo Koo

The Doctoral Dissertation
submitted to the Department of Medicine
the Graduate School of Yonsei University
in partial fulfillment of the requirements for the degree
of Doctor of Philosophy

Jeong Min Kim

December 2014

This certifies that the Doctoral Dissertation
of Jeong Min Kim is approved.

Thesis Supervisor: Bon-Nyeo Koo

Thesis Committee Member#1: Jong Eun Lee

Thesis Committee Member#2: Chan Young Shin

Thesis Committee Member#3: Kyung-Yul Lee

Thesis Committee Member#4: Seung-Soo Chung

The Graduate School
Yonsei University

December 2014

ACKNOWLEDGEMENTS

First and foremost, I would like to thank Professor Bon-Nyeo Koo for her guidance and support. This thesis would simply not be possible without her warm advice and encouragement.

I am deeply grateful to Professor Jong Eun Lee for generously providing her knowledge and guidance throughout the course of the experimental study for this thesis. I also wish to express my gratitude Jae Hoon Lee and So Yeong Cheon for their help in collecting data for this thesis.

Last but not least, I thank my family for their unfailing love and support. A special thanks to my mother-in-law for her invaluable support and love. I cannot imagine trying to accomplish such a task without her endless sacrifices to take care of my babies. Most importantly, I wish to thank my husband for his generosity and dedication during my years of graduate study.

<TABLE OF CONTENTS>

LIST OF FIGURES

ABSTRACT

The anti-inflammatory effects of agmatine
on transient focal cerebral ischemia in diabetic rats
Jeong Min Kim

Department of Medicine
The Graduate School, Yonsei University

(Directed by Professor Bon Nyeo Koo)

Background: Diabetes mellitus is a metabolic disorder associated with structural and functional alterations of various organ systems, including the central nervous system. The aim of the present study was to investigate the neuroprotective effect of agmatine (AGM) on cerebral ischemic damage in diabetic rats.

Method: Normoglycemic (n = 30) and streptozotocin-induced diabetic rats (n = 82) were subjected to 30 minutes of suture occlusion of the middle cerebral artery (MCAO) followed by reperfusion. Thirty-nine diabetic rats were treated with AGM (100 $mg \cdot kg^{-1}$, intraperitoneal) immediately after 30 minutes of MCAO. Modified neurological examination and rotarod exercise were performed to evaluate motor function. Brain infarct volume was assessed by triphenyl tetraxolium chloride staining and microPET imaging. Western blot and immunohistochemical analysis were performed to determine the expression of inflammatory cytokines in ischemic brain tissue. Real-time PCR (RT-PCR) was performed to measure the mRNA expression of high-mobility group box 1 (HMGB1), Receptor for Advanced Glycation Endproducts (RAGE), Toll-like Receptor (TLR)2, and TLR4.

Result: AGM post-treatment improved the neurobehavioral activity and motor

function of diabetic MCAO rats at 24 and 72 hours after reperfusion. The infarct size was reduced in AGM-treated diabetic rats compared with diabetic rats without AGM post-treatment ($p < 0.01$). Immunohistochemical analysis showed that AGM treatment significantly decreased the expression of inflammatory cytokines in diabetic MCAO rats at 24 and 72 hours after reperfusion ($p < 0.01$). Western blotting and RT-PCR results indicated that AGM treatment significantly decreased the expression of HMGB1, RAGE, TLR2, and TLR4 in diabetic rats at 24 and 72 hours after reperfusion ($p < 0.05$).

Conclusion: Immediate AGM treatment after 30 minutes of MCAO reduced the infarct size and neurological deficit in diabetic rats at 24 and 72 hours after reperfusion. This effect of AGM was associated with modulation of the post-ischemic neuronal inflammation cascade.

Key words: agmatine, diabetes, inflammation, innate immunity, ischemia-reperfusion injury

The anti-inflammatory effects of agmatine on transient focal cerebral ischemia in diabetic rats

Jeong Min Kim

Department of Medicine
The Graduate School, Yonsei University

(Directed by Professor Bon-Nyeo Koo)

I. INTRODUCTION

Ischemic stroke is the leading cause of long-term disability and death worldwide.[1,2] Such disabling and frequently fatal event casts substantial burden on not only family members but also the medical professionals who care for stroke victims.[1]

Diabetes mellitus (DM) is an important risk factor for ischemic stroke. Worldwide, 347 million people have DM,[3] either the type 1 or 2 forms being the most typical.[4] In a meta-analysis of prospective studies, which included 530,083 participants, the reported hazard ratio for ischemic stroke was 2.3 (95% CI, 2.0–2.7) in people with DM compared to those without DM.[5] Tureyen *et al* reported that brain damage and inflammation were exacerbated in Type 2 diabetic mice that were subjected to focal ischemia.[6] This is thought to be, at least in part, due to the increased neuroinflammation found in patients diagnosed with DM, compared with those without DM.[7] The increased level of inflammation has been attributed to the effects of poorly controlled DM which triggers NF-κB activation and the release of pro-inflammatory cytokines.[8] NF-κB can be activated protein kinase C,[9] through either the aldose reductase pathway,[10] or ligand binding to the advanced glycation end-products receptors (RAGE).[11] These pathways are all activated by hyperglycemia in microglia.[9-11]

Cerebral ischemia is a condition of complex pathology that includes

several inflammatory events, such as aggregation of inflammatory cells and upregulation of cytokines. The immune system participates in ischemic brain damage and the damaged brain, in turn, exerts an immunosuppressive effect that promotes fatal infections that threaten survival after stroke. Inflammatory signaling is involved in all stages of the ischemic cascade, from the early damaging events triggered by arterial occlusion to the late regenerative processes underlying post-ischemic tissue repair.[12] An crucial component of this response is the activation of the innate immune system.[13] Numerous studies have reported that high-mobility group box 1 (HMGB1) is released from neurons early after ischemic injury. HMGB1 plays a key role in the homeostatic regulation of brain functions and actively participates in neuropathology and neuroinflammatory responses.[14] In patients with ischemic stroke, the serum or plasma levels of HMGB1 wasdramatically higher compared with age and sex matched controls.[15,16]

Agmatine (AGM) is a locally synthesized, endogenous agonist of the imidazoline receptor, a non-catecholamine ligand for α2 adrenergic receptors, and may act as a neurotransmitter.[17] AGM treatment reduces infarct area in a mouse model of transient focal cerebral ischemia and protects cultured neurons from ischemia-like injury *via* the nitric oxide synthesis pathway.[18] Fairbanks *et al* have reported that AGM significantly reduces the pain induced by inflammation, neuropathy, and spinal cord injury.[19] However, much uncertainty still exists about the relationship between AGM and the anti-inflammatory mechanism of neuroprotection after ischemic injury.

This study investigated the neuroprotective effect of AGM post-treatment on cerebral ischemic damage in streptozotocin-induced diabetic rats subjected to 30 minutes of middle cerebral artery occlusion (MCAO). The effects of AGM on the inflammatory cascade, including the innate immunity of neuronal cells, after ischemic damage were also evaluated.

II. MATERIALS AND METHODS

Animal preparation

All animal procedures were performed according to a protocol that was approved by the Yonsei University Animal Care and Use Committee and was in accordance with National Institutes of Health guidelines for care and use of laboratory animals. A total of 112 adult male Sprague–Dawley rats, aged 8–10 weeks and weighing 280–320 g, were obtained from Orientbio Inc. (Seongnam, GyeonGi-Do, Korea) for this study. Rats were allowed free access to food and water before and after surgery.

Diabetic modeling

DM was induced in 8-week-old Sprague-Dawley rats by a single intraperitoneal injection of streptozotocin (STZ, 60 $mg \cdot kg^{-1}$ dissolved in 0.1 mM sodium citrate, pH 4.5; Sigma-Aldrich, St. Louis, MO, USA). Three days after STZ injection, blood samples were collected from the tail vein of rats which were fasted for 12 h. The blood glucose levels were measured using a glucometer (One Touch Ultra LifeScan, Milpitas, CA, USA). DM was defined as blood glucose >350 $mg \cdot dL^{-1}$. Animals were used 4 days after without any insulin supplements.

The Middle Cerebral Artery Occlusion Model and Grouping

The experimental middle cerebral artery occlusion (MCAO) model was generated as previously described.[20] Under an operating microscope, the right common carotid artery (CCA), external carotid artery (ECA), and internal carotid artery (ICA) were exposed through a midline incision. The ECA was ligated, coagulated, and cut down just proximal to the lingual and maxillary artery branches. All other branches of the ECA were coagulated and transected. The ICA was then isolated from the vagus nerve to avoid damage. A 4-0 monofilament nylon suture (Dermalone, United States Surgical, CT, USA) with

a flame-rounded head was inserted through the ICA via a small incision in the ECA stump. The distance from bifurcation of the CCA to the tip of the suture was approximately 18.5 mm in all rats, which is consistent with published descriptions of the MCAO model. Cerebral blood flow was monitored by laser Doppler flowmetry (LDF, Omega flow, FLO-C1, Neuroscience, Tokyo, Japan) using a flexible probe placed in the cortical areas that are supplied by the MCA (2 mm posterior and 6 mm lateral to bregma). After the MCA occlusion by the thread insertion, rats that did not show a cerebral blood flow reduction of at least 70% were excluded from the experiment. After 30 min of occlusion, the thread suture was withdrawn, the skin was sutured, and the rats were allowed to recover. All rats were sacrificed 24 or 72 hours after reperfusion.

Rats were allocated into 6 groups: (1) M: 30 minutes of MCAO, followed by 24 hours of reperfusion (n = 15) or 72 hours of reperfusion (n = 15) in normoglycemic rats; (2) D-M: 30 minutes of MCAO, followed by 24 hours of reperfusion (n = 22) or 72 hours of reperfusion (n = 21) in diabetic rats; and (3) D-M-A: 30 minutes of MCAO with an immediate intraperitoneal injection of AGM (100 $mg \cdot kg^{-1}$ dissolved in saline, Sigma, St. Louis, MO, USA), followed by 24 hours of reperfusion (n = 19) or 72 hours of reperfusion (n = 20) in diabetic rats. A researcher performed randomization before MCAO and prepared the study drug. Another researcher who was blinded to the treatment group performed the MCAO procedure and administered the study drug.

AGM was injected at the beginning of reperfusion. The dose of AGM in this study was based on the previous studies.[20] Previously, we have reported a successful reduction in both infarct area and brain edema with 100 $mg \cdot kg^{-1}$ AGM in a brain ischemia model.[20] These results suggested that 100 $mg \cdot kg^{-1}$ could be an efficient AGM dose to reverse the changes during an ischemic insult *in vivo*.

Neurobehavioral Assessment

Animals were examined for neurological deficits 24 hours after reperfusion by an investigator who was blind to the identity of the groups using 6 tests developed and described by Garcia *et al.*[21] The score assigned to each rat at the completion of the evaluation was the sum of all 6 test scores: (1) spontaneous activity; (2) symmetry in the movement of the 4 limbs; (3) forepaw outstretching; (4) climbing; (5) body proprioception; and (6) response to vibrissae touch. The final maximum neurological score was 18. The rotarod test was used to assess the recovery of impaired motor function after MCAO (n = 15 in each group). The accelerating rotarod test (ENV-577, Med Associates Inc., Geordia, VT, USA) was carried out as described by Hunter *et al*.[22] with a slight modification. Exercise time was measured as the amount of time the animal remained on an accelerating rotarod cylinder. The speed was increased from 4–40 rpm within 5 minutes. The trial ended if the animal fell off the rungs or gripped the device and spun around for two consecutive revolutions without attempting to walk on the rungs. The exercise time for each rat was measured 5 times per day just before MCAO, and 24 and 72 hours after MCAO.

Measurement of Brain Infarct Volume

After 24 or 72 hours of reperfusion, animals were anesthetized with a mixture of Zoletil® and Rompun®, and were decapitated. The brains were quickly isolated and sectioned into serial 2 mm thick coronal slices. Brain infarct volume was determined by 2, 3, 5-triphenyl tetraxolium chloride (TTC) (Sigma-Aldrich, St. Louis, MO, USA) staining using a computer-assisted image analysis system (Optimas ver 6.1, Optimas, Bothell, WA, USA). The result was corrected for the presence of edema using a previously published method.[23] The infarct volume was calculated in mm^3 by integrating the infarct sizes for each slice which contained infarcted brain tissue. The edema volume was calculated by subtracting the volume of the contralateral hemisphere from the ipsilateral

hemisphere.

Biochemical Assessment

Immunohistochemistry

Five rats from each group were deeply anesthetized and transcardially perfused with 4% paraformaldehyde in phosphate-buffered saline (PBS) 24 or 72 hours after MCAO. The brain was quickly removed and post-fixed overnight in 4% paraformaldehyde at 4 ℃. Paraffin sections (4 μm) were dewaxed and rehydrated. Endogenous peroxidase was blocked using 0.1% H_2O_2 in PBS for 30 minutes. The sections were pre-incubated in 5% normal goat serum in PBS for 30 minutes and incubated overnight at 4 ℃ with the following primary antibodies: anti-NF-κB (Santa Cruz Biotechnology, Santa Cruz, CA, USA), anti-IL-1β (Santa Cruz Biotechnology, Santa Cruz, CA, USA), and anti-TNFα (Chemicon, Temecula, CA, USA). Antigens were detected with 3,3-diaminobenzidine (DAB) (Vector Laboratories, Burlingame, CA, USA) using an Elite ABC kit (Vector Laboratories, Burlingame, CA, USA) and hematoxylin (Sigma-Aldrich, Saint Louis, MO, USA) was used as a counterstain. The samples were incubated in hematoxylin for 5 minutes and dehydrated through 70%, 95%, and 100% graded ethanol. The sections were mounted with Vectashield mounting media (Vector Laboratories, Burlingame, CA, USA). Staining was observed under a microscope with a digital camera.

Immunoreactive cells in the cortex and striatum region were counted in 5 coronal sections (bregma, −0.8 to 1.2 mm) per brain in 5 rats per group using a CAST Grid system (Computer-Assisted Stereological Toolbox; version 2.1.4 Olympus, Denmark A/S, Ballerup, Denmark). The number of positive cells was estimated as the number of counted cells divided by the sampling fraction. Within the cortex and striatum boundaries, counting frames of 48.6 × 36.1 μm in size were systematically and randomly sampled on the first counting area and moved through all counting areas until the entire delineated area was sampled.

Actual counting was performed using a ×100 oil objective lens. The estimate of the total number of positive cells was calculated according to the optical fractionator formula. The data are expressed as the total number of positive cells and presented as mean ± standard error of the mean (SEM) within the investigated region.

Immunofluorescent staining

The samples were fixed with 3.7% formaldehyde and sectioned at 20-μm thickness by a cryotome. Samples were immunostained with anti-Iba-1 (1:100, Abcam, Cambridge, UK) and anti-NF-κB (1:60, Santa Cruz Biotechnology, Santa Cruz, CA, USA). After washing with PBS, samples were incubated with Rhodamine- and FITC-conjugated secondary antibodies (1:200, Millipore, Bedford, MA, USA), and counterstained with DAPI. Immunolabeled cells were observed under an LSM 700 confocal laser scanning microscope (Carl Zeiss, Thornwood, NY, USA). The immunofluorescent intensity present on each slide was measured using ImageJ. Relative intensity was divided by the number of cells. Four images from the ipsilateral and contralateral cortex and striatum were used in this analysis.

Immunoblotting Assay

Five rats from each group were killed 24 or 72 hours after MCAO. The brain was quickly removed and the bilateral hemispheres were dissected. All procedures were carried out while maintaining the brain on ice. The dissected tissue was either frozen or used immediately. Tissue was homogenized in a modified RIPA-buffer [50 mM Tris-HCL pH 7.4, 150 mM NaCl, 1% NP-40, 0.25% sodium deoxycholate, complete protease inhibitor cocktail (Sigma-Aldrich)] and incubated for 20 minutes on ice. After 15 minutes of centrifugation (13,000 rpm, 4 ℃), the protein concentration of the supernatant was determined using a bicinchoninic acid-containing reagent (BCA Protein

Assay Reagent kit, Pierce, Rockford, IL, USA). Samples (50 µg protein/well) were separated on an 8% acrylamide gel using sodium dodecyl sulfate-poly-acrylamide gel electrophoresis. The gels were then electro-transferred onto polyvinylidene difluoride membranes (PVDF, Millipore, Bedford, MA, USA). Membranes were blocked with 5% nonfat skim milk (dissolved in tris buffered saline with 0.1% Tween 20, TBST) for 1 hour at room temperature and then incubated overnight at 4 ℃ with the following antibodies: anti-β-actin (Abcam, Cambridge, MA, USA), anti-NF-κB (Santa Cruz Biotechnology), anti-IL-1β (Santa Cruz Biotechnology), anti-TNFα (Chemicon), anti-RAGE (Abcam), anti-GAPDH (Santa Cruz Biotechnology), anti-HMGB1 (Abcam), anti-Histon (Abcam), anti-TLR4 (Abcam), and anti-TLR2 (Novus Biologicals, Littleton, CO, USA). The membranes were extensively washed with TBST and incubated with horseradish peroxidase (HRP) conjugated anti-rabbit, mouse, or goat IgG secondary antibodies. The bands were visualized with enhanced chemiluminescence reagents (ECL Plus; Amersham Biosciences, Piscataway, NJ, USA) and developed using x-ray films (Kodak, Rochester, NY, USA). The optical density of the bands were quantified using a computer-associated image analysis system (National Institutes of Health, Image J). Target proteins were normalized to β-actin, GAPDH, and Histon.

Real-time PCR

mRNA expression analysis of TLR4, TLR2, HMGB1, and RAGE were performed as reverse transcription with total RNA, and complementary DNA (cDNA) were synthesized by polymerase chain reaction (PCR). The primers that were used are as follows: TLR4: forward, 5’-CTT GGT TGA ATA AGG GAT GTC AT- 3’; reverse, 5’- GAA GCT ACT GCA GGA GG TA-3’; HMGB1: forward, 5’-TCC TTC GGC CTT CTT CTT GT-3’; reverse, 5’-CTC TCC TAG TTT CTT CGC AAA A-3’; forward, 5’-TGA TGC TGC CAT TCT CAT TC-3’;

reverse, 5'-CGC CGC TCT CAG ATT TAC CC-3'; RAGE: forward, 5'-AGG ACC AGG GAA CCT ACA GC-3'; reverse, 5'-CCT GAT CCT CCC ACA GAG C-3'. The PCR was performed with following condition: initial denaturation at 95 ℃ for 5 min, amplification by 39 cycles of 10 sec at 95 ℃, 30 sec at 60 ℃, and for 5 min, amplification at 72 ℃ for 10 sec. The target genes were analyzed with CFX manager software from Bio-Rad (Bio-Rad Laboratories, Berkeley, CA, USA). The expression of mRNA was normalized to β-actin.

Micro positron emission tomography (PET)

Twenty-four hours after reperfusion, each rat was given an intravenous (IV) injection of ^{18}F-fludeoxyglucose (FDG), a standard radiotracer *via* the tail vein for 65 minutes. Rats were anesthetized with 2% isofluorane in oxygen in a chamber. After this, rats were scanned using a Siemens Inveon microPET scanner. Optimal PET acquisition time was 20 minutes. Serial autoradiographic images were obtained after brain uptake of ^{18}FDG and evaluated using 3D ordered-subset expectation maximization (OSEM). The region of interest (ROI) template included 58 regions according to a rat template (data courtesy of Wynne Schiffer). Co-registration and ROI analysis were performed using Powell's convergence optimization method (PMOD) software (http://www.pmod.com). The measurements obtained from ROIs on the ipsilateral side were divided by the contralateral measurements. This provided a regional quantification of relative changes in cerebral blood flow or glucose uptake in the same animal.

Statistical Analysis

All statistical analyses were performed using SPSS software (version 20.0, SPSS Inc., Chicago, IL). Most of the statistical assessments were performed using 1-way analysis of variance (ANOVA), followed by post hoc

multiple comparison tests (Tukey). The neurological scores were compared by Kruskal-Wallis and 1-way ANOVA, and multiple comparison tests using the Dunn method. All data are presented as mean ± SEM. Statistical significance refers to results where $p < 0.05$ and $p < 0.01$ were obtained.

III. RESULTS

Body weight and blood glucose in the STZ-induced diabetic rat

The mean body weight of diabetic rats in both the D-M group and the D-M-A group was reduced after STZ injection and was lower than the mean body weight in the M group throughout the experiment period ($p < 0.05$, Figure 1A). After STZ injection, blood glucose level increased and was 410.8% higher than the that of the normal rats three days later, and remained higher until the day of surgery (416.8 ± 13.2 *versus* 101 ± 5.8 mg/dL). Treatment with AGM 1 week after STZ injection induced a mild decrease in the blood glucose level in diabetic rats. The lowering of plasma glucose lasted from 30 minutes to 6 hours and reached its maximum at 2 hours (416.8 ± 13.2 *vs.* 337.0 ± 7.7 mg/dL, $p < 0.05$). Twenty-four hours after AGM injection, no difference in the mean plasma glucose level of the diabetic rats were seen either treated with or without AGM (392.8 ± 15.2 *vs.* 419.8 ± 12.4 mg/dL, Figure 1B).

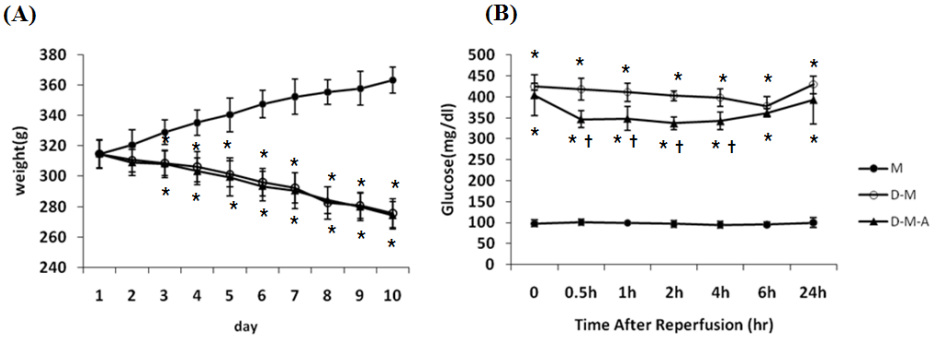

Figure 1. The changes in body weight and blood glucose

Body weight (A) and blood glucose (B) were assessed in the M, D-M, and D-M-A groups. (A) Diabetes mellitus (DM), induced by streptozotocin (STZ), resulted in significant weight loss with and without AGM treatment, before and after MCAO. (B) After the STZ injection, blood glucose levels were increased and remained high until the day of surgery. Treatment with AGM after STZ injection induced a mild decrease in blood glucose level compared with the D-M group. Data are presented as mean ± SEM (n = 10 per group). MCAO: middle cerebral artery occlusion; AGM: agmatine; M: normoglycemic rats subjected to MCAO; D-M: diabetic rats subjected to MCAO; D-M-A: diabetic rats post-treated with AGM immediately after reperfusion. *$p < 0.05$ versus the M group (A), *$p < 0.01$ versus the M group, and †$p < 0.05$ versus the D-M group (B).

Regional Cerebral Blood Flow

Regional cerebral blood flow during occlusion and the first 5 minutes of reperfusion were not significantly different among the 3 groups.

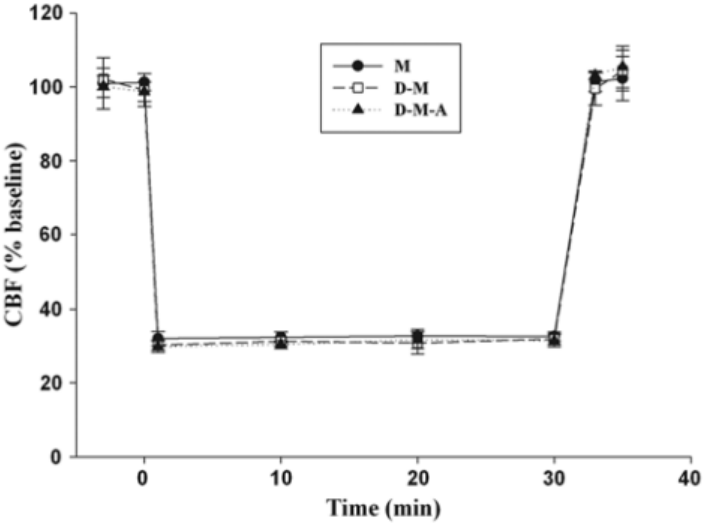

Figure 2. Regional cerebral blood flow (rCBF) in normoglycemic and diabetic rats

The rCBF was measured using a laser-Doppler flowmetry before, during, and after middle cerebral artery occlusion. There was no difference in rCBF between groups. The data are presented as mean ± SEM (n = 5 per group). M: normoglycemic rats subjected to MCAO; D-M: diabetic rats subjected to MCAO; D-M-A: diabetic rats post-treated with AGM immediately after reperfusion.

Agmatine reduced infarct volume

To measure infarct volume, TTC staining was performed at 24 and 72 hours after reperfusion. The mean infarct size of rats subjected to 30 minutes of MCAO was larger in the D-M group compared with the M group at 24 and 72 hours after reperfusion (all $p < 0.01$). The mean infarct volume was smaller in the D-M-A group compared with the D-M group at 24 and 72 hours after reperfusion. (all $p < 0.01$) Agmatine significantly reduced the infarct size in diabetic rats subjected to 30 minutes of MCAO. There was no significant difference in the infarct volume between the M and D-M-A groups at 24 and 72 hours after reperfusion (all $p > 0.05$, Figure 3).

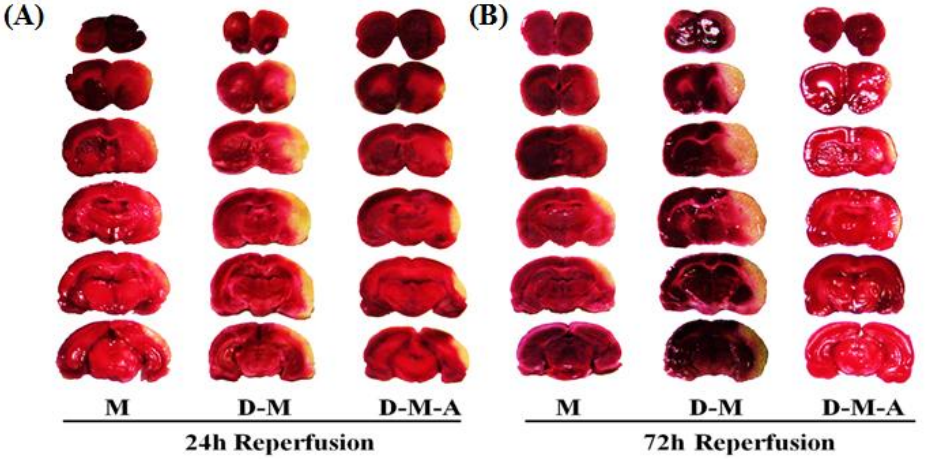

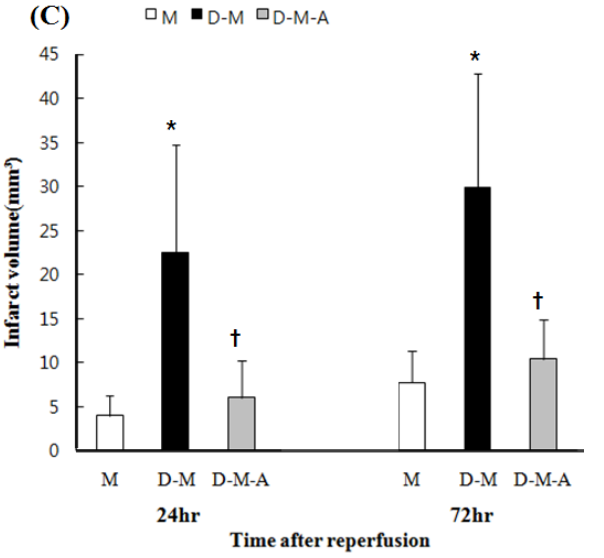

Figure 3. The effect of AGM on infarct volume

(A) Representative infarct volume was determined by staining with 2% TTC at 24 hours after reperfusion for each group. Infarct volume was larger in the D-M group compared with the M group and AGM efficiently decreased infarct volume in the D-M-A group. (B) Infarct volume in all groups was measured at 72 hours after reperfusion. (C) Quantitative data of infarct volume. The graph shows that augmented volume of infarct in the D-M-A group was reduced compared with that in the D-M group after treatment with AGM. Data were presented as mean ± SEM (n = 5 per group). TTC: 2, 3, 5-triphenyl tetraxolium chloride; M: normoglycemic rats subjected to MCAO; D-M: diabetic rats subjected to MCAO; D-M-A: diabetic rats post-treated with AGM immediately after reperfusion. *$p < 0.01$ *versus* the M group, †$p < 0.01$ *versus* the D-M group.

Agmatine preserved glucose metabolism, measured by microPET imaging

^{18}FDG microPET scans were performed according to the schedule detailed in the methods section. The ROI template included 58 regions following a standard rat template (data courtesy of Wynne Schiffer). Our hypothesis was that the MCAO would influence ^{18}FDG uptake in the ipsilateral hemisphere; therefore, we separated the template into ipsilateral versus contralateral regions. The ratio of ^{18}FDG signal between the ipsilateral and contralateral ROI was significantly lower in the D-M group compared with other groups (Figure 4).

The ^{18}FDG uptake ratio between the ipsilateral and contralateral hemisphere was inversely proportional to infarct volume. AGM significantly conserved ^{18}FDG uptake in diabetic rats subjected to 30 minutes of MCAO. There was no significant difference in ^{18}FDG uptake between the M and D-M-A groups at 24 hours after reperfusion (all $p > 0.05$, Figure 4).

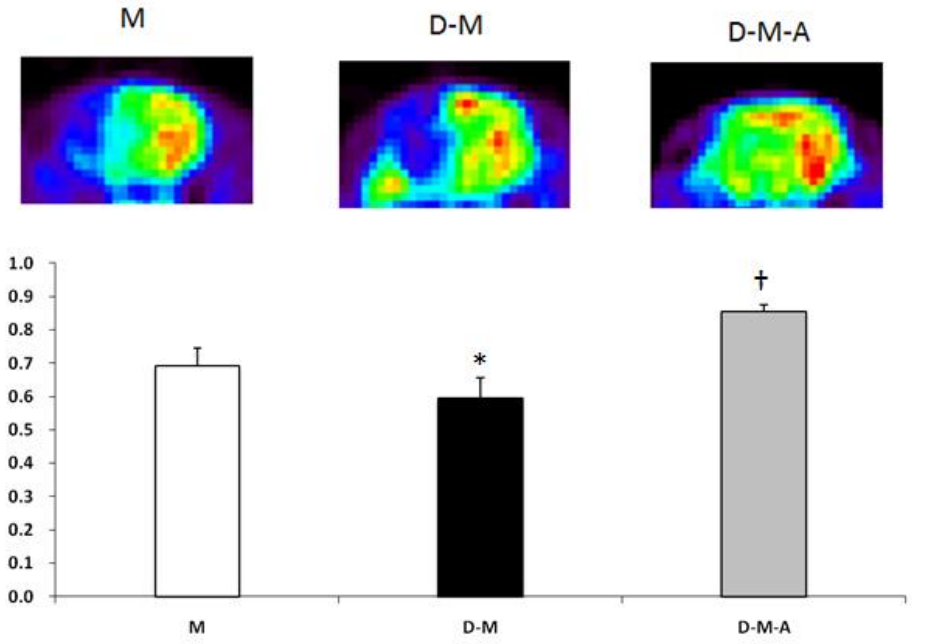

Figure 4. Preservation of glucose metabolism after treatment with AGM detected by microPET imaging.

The ^{18}FDG uptake in the region of interest (ROI) was lower in the ipsilateral hemisphere than in the contralateral hemisphere in each model. The ratio between the ipsilateral and contralateral ROI was significantly lower in the D-M group compared with the other groups. Data are presented as mean ± SEM (n = 5 per group). M: normoglycemic rats subjected to MCAO; D-M: diabetic rats subjected to MCAO; D-M-A: diabetic rats post-treated with AGM immediately after reperfusion. *p < 0.01 *versus* the M group, †p < 0.01 *versus* the D-M group.

Agmatine preserved neurological function

The rotarod test was performed to evaluate the protective properties of AGM on neurological functions (Figure 5). There was no difference in exercise time on the rotarod with accelerating speed from 4 to 40 rpm between the 3 groups before surgery. After MCAO, a marked reduction in exercise time at 24 and 72 hours after reperfusion was shown (Figure 5A). The exercise time in the D-M group was lower compared with other groups at 24 and 72 hours after reperfusion (both $p < 0.01$). The D-M-A group showed better motor performance than the D-M group at 24 and 72 hour after reperfusion. There was no significant difference in exercise time between the D-M-A group and the M group at 24 and 72 hours after reperfusion (both $p > 0.05$). The exercise time on the rotarod was longer in the D-M-A group compared with the D-M group at 24 and 72 hours after reperfusion (both $p < 0.01$).

No neurological deficit was present in any experimental animal before surgery. The modified neurological exam score was lower in the D-M group compared with the M group at 24 and 72 hours after reperfusion (both $p < 0.01$). AGM treatment improved the neurological score in the D-M-A group at 24 and 72 hours after reperfusion when compared with the D-M group ($p < 0.01$).

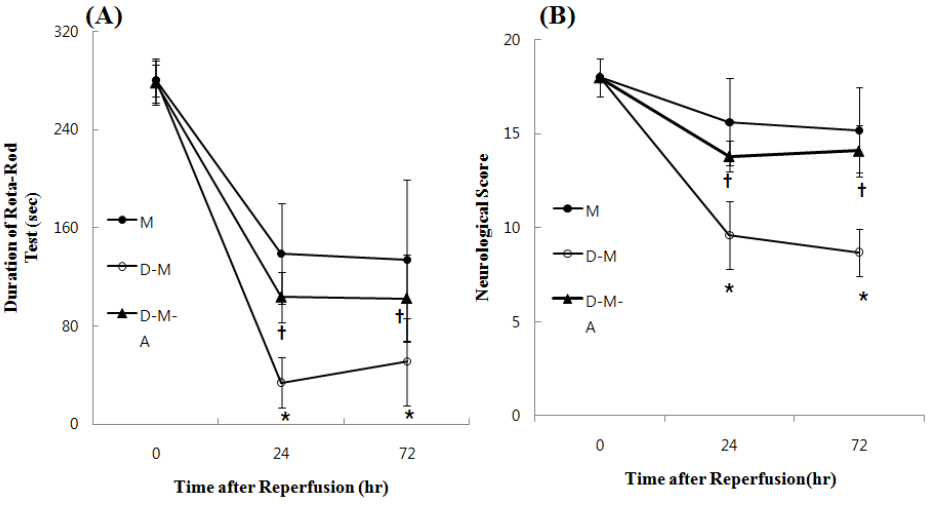

Figure 5. The ameliorating effect of AGM on neurological functional deficits

(A) The duration of time spent on the rotarod. The D-M group showed severe functional deficits; however, rats in the D-M-A group showed better functional performance at 24 and 72 h reperfusion. (B) Neurological deficits were scored using the modified neurological examination. The neurological score was lower in the D-M group compared with the M group at 24 and 72 hours after reperfusion. AGM treatment improved the neurological score more in the D-M-A group compared with the D-M group. Data are presented as mean ± SEM (n = 10 per group). M: normoglycemic rats subjected to MCAO; D-M: diabetic rats subjected to MCAO; D-M-A: diabetic rats post-treated with AGM immediately after reperfusion. *$p < 0.01$ *versus* the M group, †$p < 0.01$ *versus* the D-M group.

AGM suppressed the activation of microglia.

Many activated microglia, which were detected by Iba-1 immunoreactivity, were easily observed in the ischemic cortex and striatum in the D-M group and the M group also showed many Iba-1-positive cells. However, agmatine suppressed the activation of microglia in the D-M-A group compared with the other groups (Figure 6A and 6B). In the contralateral hemisphere, less Iba-1 immunoreactivity was observed compared with ipsilateral hemisphere (Figure 6C and 6D). In the D-M-A group, the number of Iba-1-positive cells was reduced in the cortex and striatum compared with the D and D-M groups.

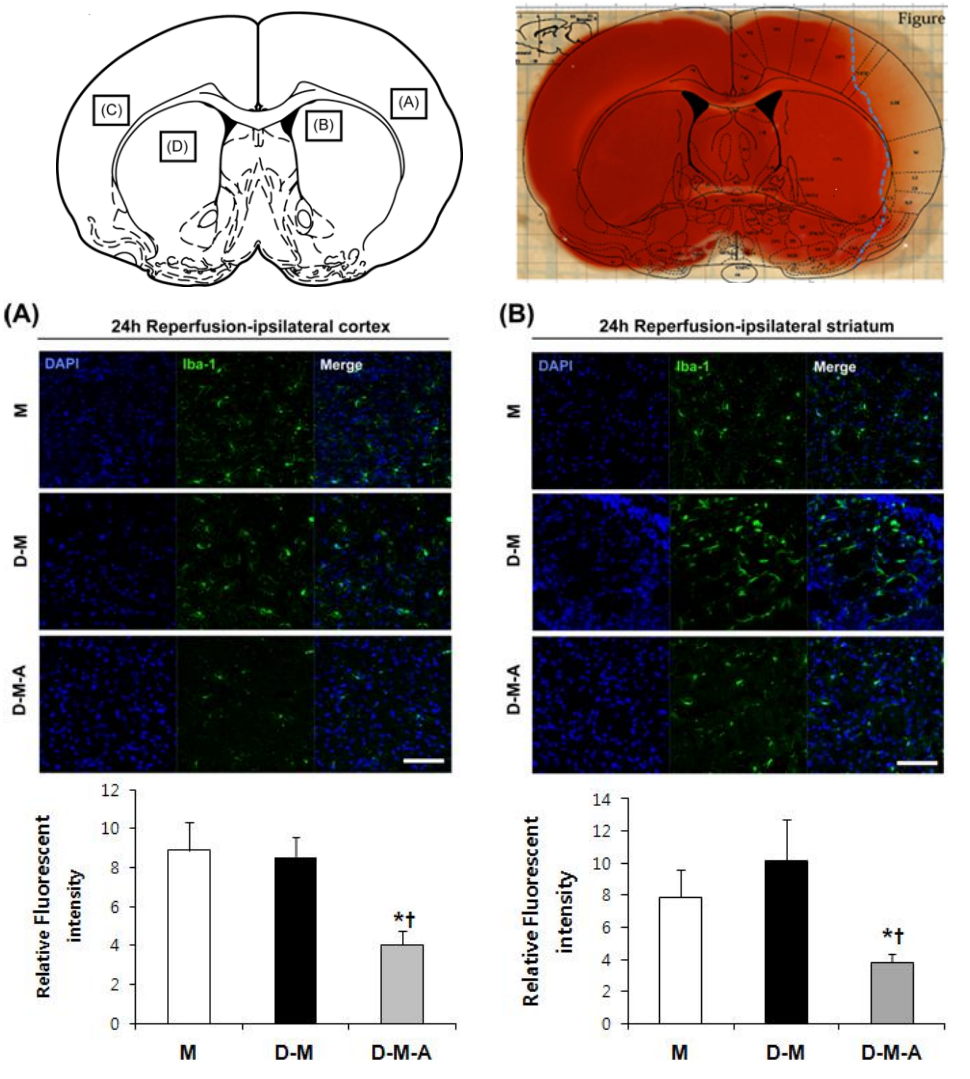
(C)
(D)
(B)
(A)
Figure
(A)
24h Reperfusion-ipsilateral cortex
DAPI
Iba-1
Merge
M
D-M
D-M-A
Relative Fluorescent intensity
12
10
8
6
4
2
0
*†
M
D-M
D-M-A
(B)
24h Reperfusion-ipsilateral striatum
DAPI
Iba-1
Merge
M
D-M
D-M-A
Relative Fluorescent intensity
14
12
10
8
6
4
2
0
*†
M
D-M
D-M-A

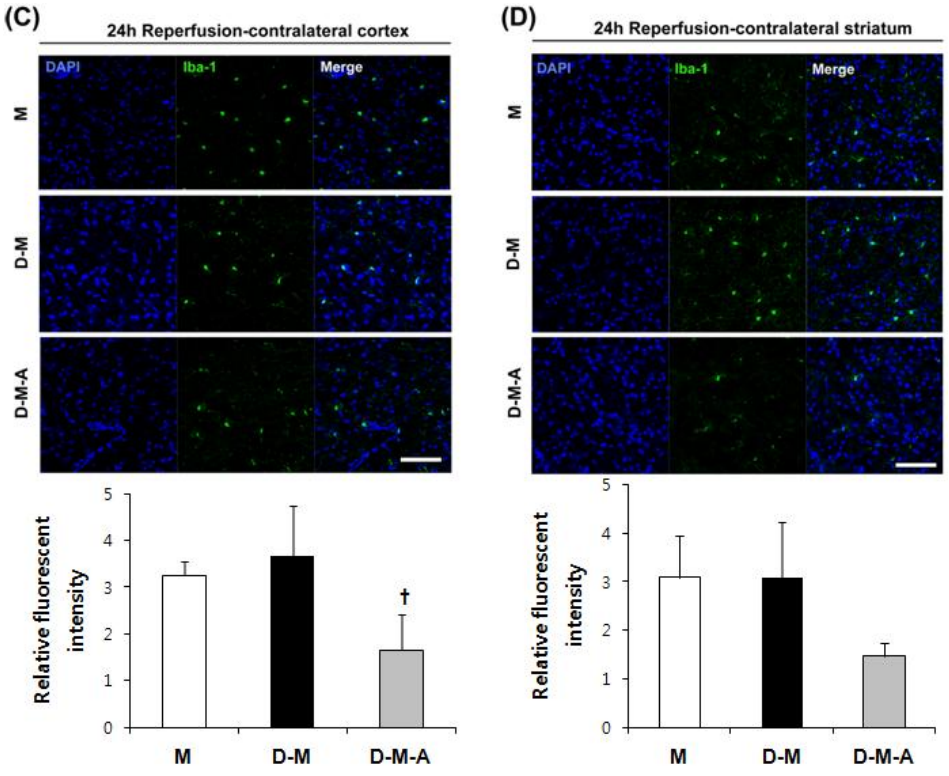

Figure 6. The distribution of microglia after treatment with AGM

(A and B) After ischemic injury, many Iba-1-positive cells (green) were observed in ipsilateral cortex and striatum in all groups. In the M and D-M groups, high levels of Iba-1 expression were found in the ischemic cortex. The relative intensity of immunofluorescence was divided by the total number of cells. (A) There were a greater number of Iba-1-positive cells in the D-M group compared with the M group. In contrast, after agmatine treatment, the number of Iba-1-positive cells was reduced in the ischemic cortex in the D-M-A group. (B) In the ischemic striatum, Iba-1 expression had the same pattern as in the ischemic cortex. (C and D) In the contralateral hemisphere, Iba-1 expression had the same pattern compared with the ipsilateral hemisphere. However, the expression of Iba-1 was reduced in the contralateral cortex (C) and striatum (D) compared with ipsilateral striatum and cortex. DAPI was used as a counterstain.

Scale bar = 100 μm). M: normoglycemic rats subjected to MCAO; D-M: diabetic rats subjected to MCAO; D-M-A: diabetic rats post-treated with AGM immediately after reperfusion. *$p < 0.01$ versus the M group, †$p < 0.01$ versus the D-M group.

AGM ameliorates the expression of NF-κB, IL-1β, and TNF-α and microglial activation

The most studied cytokines related to inflammation in acute ischemic stroke are tumor necrosis factor-alpha (TNF-α) and the interleukins (such as IL-6). TNF-α can activate nuclear factor-κB (NF-κB) in microglia, thus increasing the production of cytokines from microglia. To evaluate the expression of pro-inflammatory cytokines, we compared the number of immunoreactive cells using a CAST Grid system. In our study, the immunohistochemistry results demonstrated a significant increase in NF-κB (stealth arrow), a pro-inflammatory cytokine, and microglia (open arrow) in the D-M group at 24 and 72 hours after reperfusion (Figure 7A). After ischemia and reperfusion, NF-κB-positive cells and microglia were discriminated using brown dye in the ipsilateral and contralateral hemispheres of the M, D-M, and D-M-A groups. Twenty-four hours after reperfusion, more densely double positive cells were observed in the D-M group than the M group. However, after treatment with AGM, the number of merged cells was effectively reduced in the ipsilateral and contralateral hemispheres. Merged cells at 72 hours after reperfusion were augmented compared with 24 hours after reperfusion. The same patterns were found as in rats assessed 24 hours after reperfusion: strong expression of NF-κB -positive cells and microglia in the D-M group with a reduction in NF-κB and microglia-immunoreactivity in the D-M-A group (Figure 7B).

To assess whether AGM affects the nuclear translocation of NF-κB (p65), immunofluorescent staining was performed at 24 hours after ischemia

(Figure 8). In response to ischemic injury, NF-κB in the cytosol was activated and translocated into the nucleus. Z-stack images (3D image stacks) created by the confocal microscope showed that the activated form of NF-κB, NF-κB p65, was remarkably expressed in the nucleus of the M and D-M groups. In the D-M-A group, NF-κB was expressed in a peri-nuclear scattered pattern. AGM suppressed the nuclear translocation of NF-κB (Figure 8).

To investigate whether AGM downregulated the pro-inflammatory cytokine, IL-1β, and microglia, immunolabeling was conducted at 24 and 72 hours after reperfusion (Figure 9A). The number of double positive cells (IL-1β and microglia positive cells) of the ipsilateral hemisphere in the D-M group was higher compared with the M group at 24 and 72 hours after reperfusion. Efficiently reduction of the number of double positive cells was observed after AGM treatment in the ipsilateral hemisphere at 24 and 72 hours after reperfusion. There was no difference in the number of merged cells between the M and D-M-A groups. The number of merged cells in the contralateral hemisphere 24 hours after reperfusion was similar at 72 hours after reperfusion in all 3 groups (Figure 9B).

TNF-α and microglia immunoreactivity was visualized at 24 and 72 hours after reperfusion by using immunohistochemistry (Figure 10A). The data demonstrated that in ipsilateral hemisphere at 24 and 72 hours after reperfusion, double positive cells (TNF-α and microglia positive cells) were not noticeably expressed in the M group. However, TNF-α expression, microglial activation, and double positive cells were significantly increased in the D-M group. After treatment with AGM, TNF-α expression and microglia were downregulated in the D-M-A group.

The contralateral hemispheres of all 3 groups showed the same pattern as ipsilateral hemisphere (Figure 7B, 9B, and 10B). As shown in the figures, inflammatory cytokines were increased in the D-M group in the contralateral hemisphere compared with the other groups.

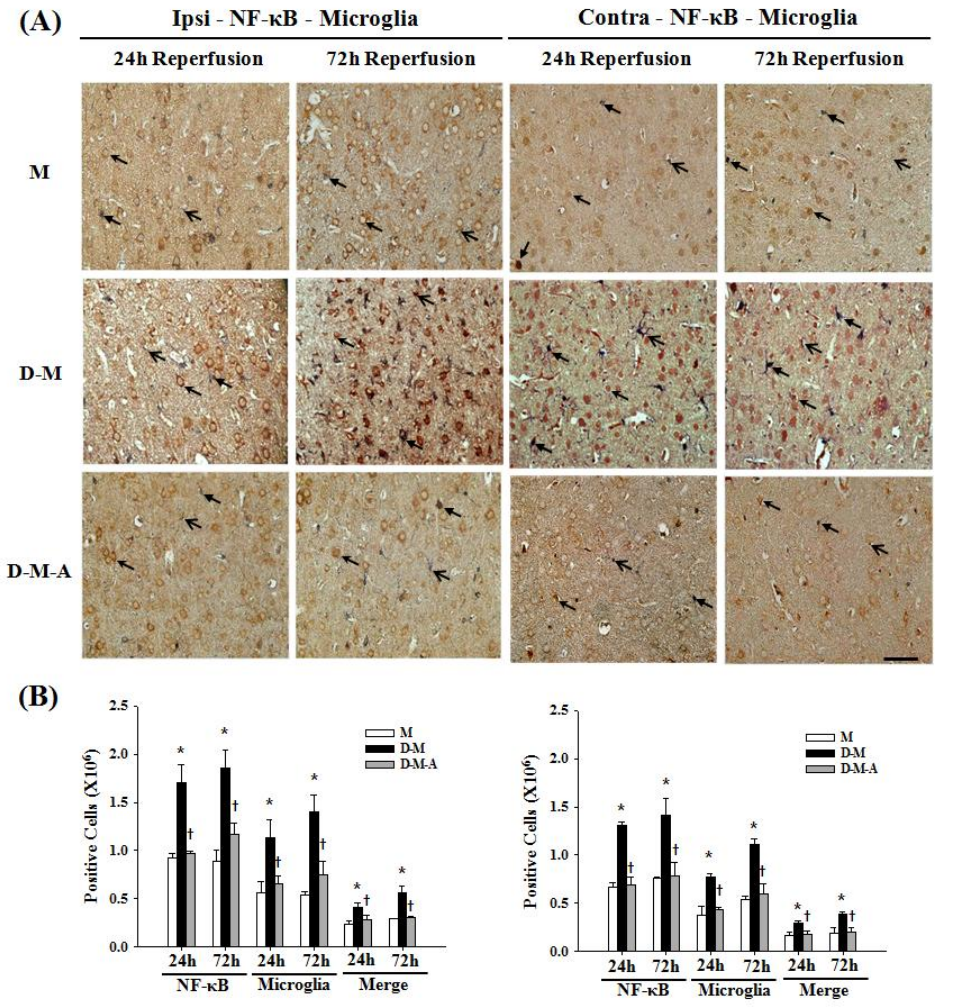

Figure 7. Decreased NF-κB expression and microglia number after treatment with AGM

(A) Double staining for NF-κB (stealth arrow) and microglia (open arrow) was performed at 24 h and 72 h after reperfusion in all 3 groups. (B) The quantitation graph presents the number of NF-κB, microglia, and merged cells were increased in ipsilateral (left) and contralateral (right) hemisphere of the D-M group compared with in the M and D-M-A groups. Data were presented as mean ± SEM (n = 5 per group). M: normoglycemic rats subjected to MCAO;

D-M: diabetic rats subjected to MCAO; D-M-A: diabetic rats post-treated with AGM immediately after reperfusion. *p < 0.05 *versus* the M group, †p < 0.05 *versus* the D-M group.

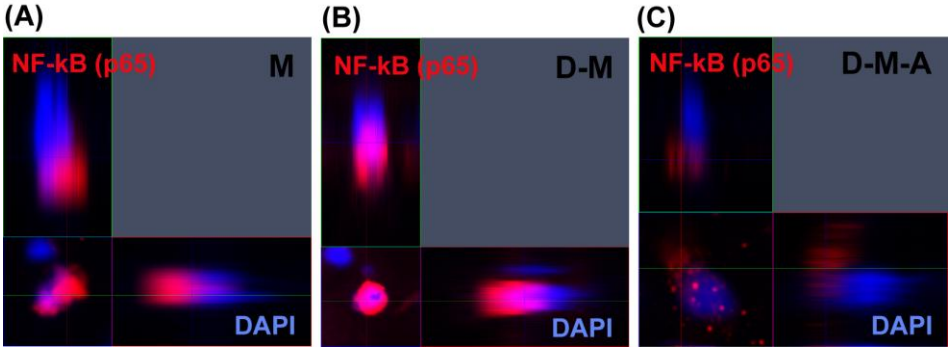

Figure 8. The activation of NF-κB (p65) after treatment with AGM

(A and B) Activation of NF-κB (red) was confirmed with immunohistochemistry. After ischemic insult, NF-κB was highly expressed in the ischemic areas. In the M and D-M groups, the activated form of NF-κB p65 was intensely expressed and NF-κB p65 was translocated into the nucleus. (C) Agmatine inhibited the translocation of NF-κB p65 into the nucleus, compared with the M and D-M groups. DAPI was used as a counterstain.

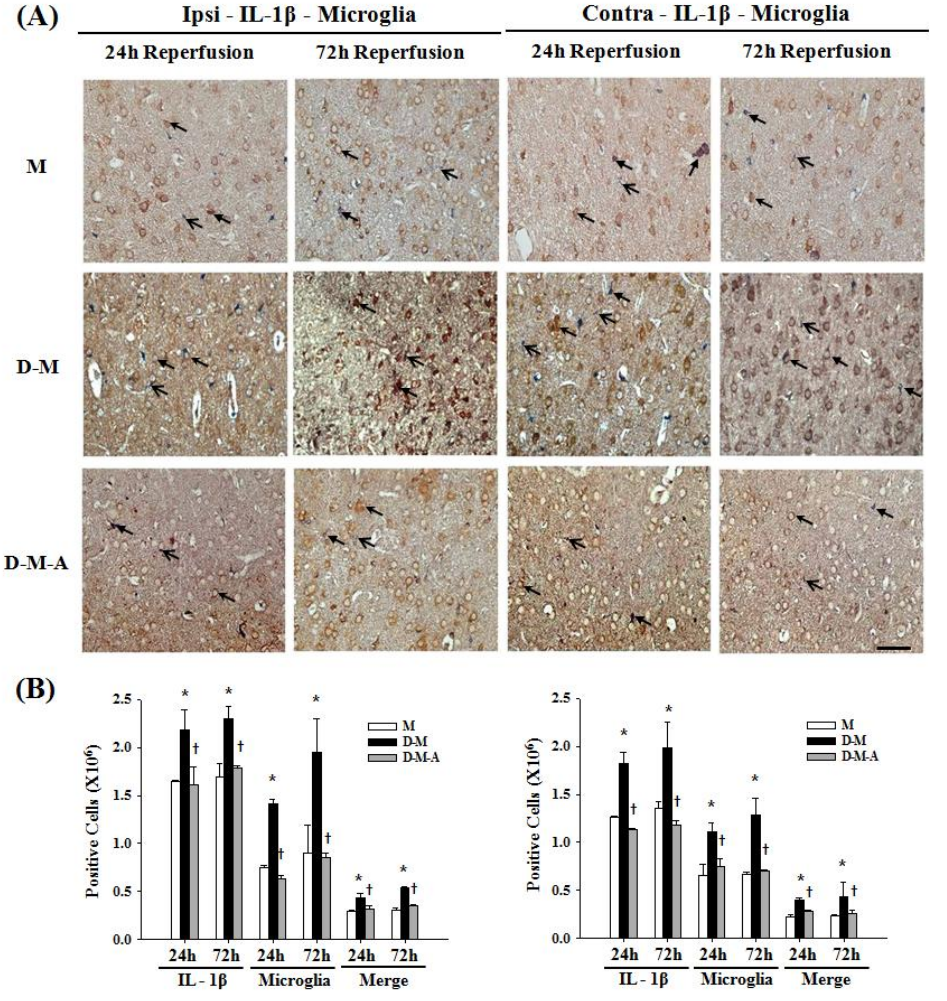

Figure 9. Decreased IL-1β expression and microglia number after treatment with AGM

(A) The IL-1β expression (stealth arrow), and microglia (open arrow), were observed by immunohistochemistry at 24 and 72 hours after reperfusion in all 3 groups. (B) The graph of the number of IL-1β positive cells, microglia, and merged cells were upregulated in contralateral (right) and ipsilateral (left) hemisphere in the D-M group, compared with in the M and D-M-A groups. Data are presented as mean ± SEM (n=5 per group). M: normoglycemic rats subjected to MCAO; D-M: diabetic rats subjected to MCAO; D-M-A: diabetic

rats post-treated with AGM immediately after reperfusion. *$p < 0.05$ *vs*. the M group, †$p < 0.05$ *versus* the D-M group.

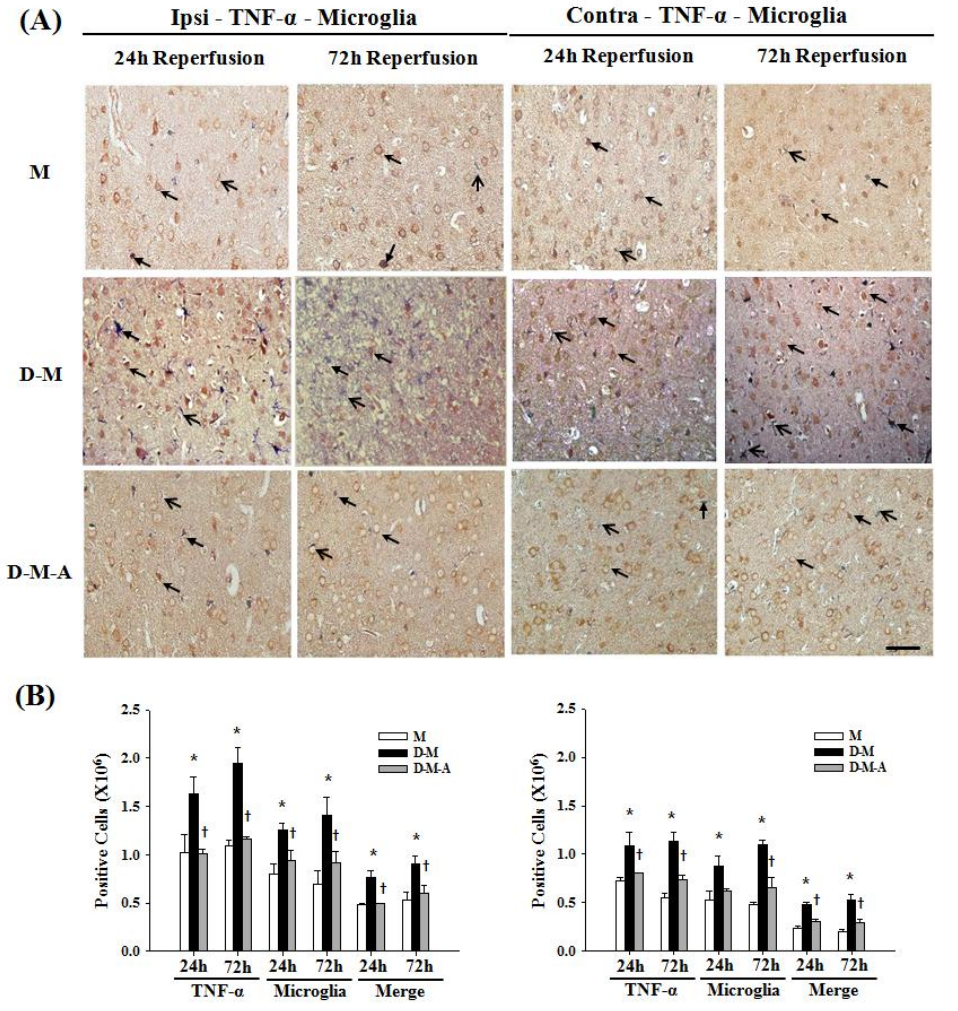

Figure 10. Decreased TNF-α expression and microglia after treatment with AGM.

(A) The TNF-α expression (Stealth arrow), and microglia (open arrow) were detected by immunohistochemistry at 24 and 72 hours after reperfusion in all 3 groups. (B) The number of TNF-α positive, microglia, and double positive cells were increased in the ipsilateral (left) and contralateral (right) hemisphere in the

D-M group compared with the M and D-M-A groups. Data are presented as mean ± SEM (n = 5 per group). M: normoglycemic rats subjected to MCAO; D-M: diabetic rats subjected to MCAO; D-M-A: diabetic rats post-treated with AGM immediately after reperfusion.*$p < 0.05$ *versus* the M group, †$p < 0.05$ *versus* the D-M group.

AGM suppressed the protein levels of NF-κB, IL-1 β, and TNF-α

To examine whether AGM affects the protein expression of NF-κB, IL-1β, and TNF-α, western blot analysis was performed at 24 and 72 hours after reperfusion (Figure 11A). The protein levels of NF-κB, IL -1β, and TNF-α were significantly increased in the D-M group at 24 and 72 hours after reperfusion compared with the M group. Although rats were given the same injury as the D-M group, the AGM-treated group presented efficiently decreased protein levels of NF-κB, IL-1β, and TNF-α. These western blot results were concurrent with the immunohistochemistry results of NF-κB, IL-1β, and TNF-α. The optical density of the bands was normalized to β-actin optical density (Figure 11B).

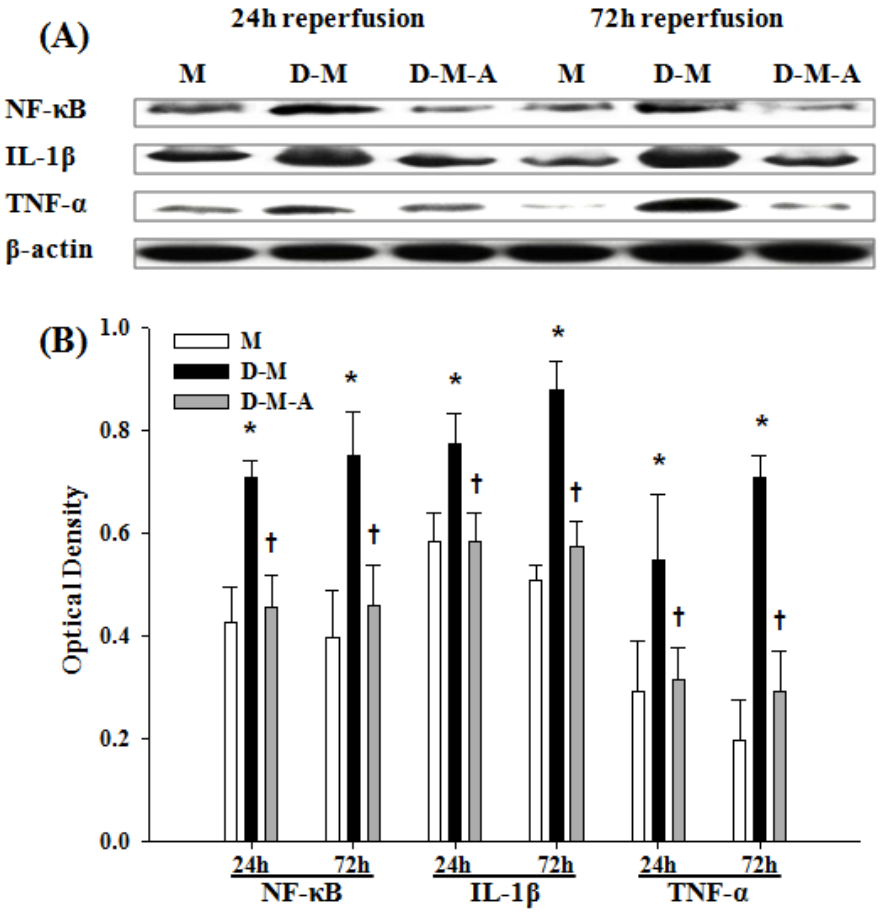

Figure 11. The protein levels of pro-inflammatory cytokines, NF-κB, IL-1β, and TNF-α after treatment with AGM at 24 hours after reperfusion

(A) Western blot analysis was performed to measure the protein levels of NF-κB, IL-1β, and TNF-α. The NF-κB band (MW: 65 kDa), IL-1β band (MW: 31 kDa), and TNF-α band (MW: 17 kDa) were detected in the ipsilateral hemisphere of rat brain. (B) The relative optical density showed elevated levels of NF-κB, IL-1β and TNF-α in the D-M group compared with the M and D-M-A groups. AGM treatment decreased the levels of NF-κB, IL-1β, and TNF-α protein. The optical density of the bands was normalized to the optical density of β-actin bands. Data are presented as mean ± SEM (n = 5 per group).

M: normoglycemic rats subjected to MCAO; D-M: diabetic rats subjected to MCAO; D-M-A: diabetic rats post-treated with AGM immediately after reperfusion. *$p < 0.05$ *versus* the M group, †$p < 0.05$ *versus* the D-M group.

AGM downregulated the protein levels of HMGB1, RAGE, TLR2, and TLR4 at 24 hours after reperfusion

HMGB1 is normally located in the nuclei; however, it translocates to the cytoplasm and/or extracellular space and mediates inflammation after exposure to damaging processes, such as ischemia and inflammation.[24] To confirm the translocation of HMGB1, subcellular fractions (the nuclear/cytosolic fraction) were obtained and examined using western blotting. It was found that cytosolic HMGB1 was highly upregulated in the ipsilateral hemisphere in the D-M group after MCAO. Relatively lower levels of nuclear HMGB1 were detected in the same group. Translocation of HMGB1 from the nucleus to the cytoplasm in the D-M-A group was downregulated compared to the D-M group. The levels of HMGB1 in the cytosol and nucleus in the M and D-M-A groups did not show any differences (Figure 12A and B).

Immunoreactivity for HMGB1 receptors, such as RAGE, TLR2, and TLR4, were seen in all 3 groups. As shown in Figure 13A, quantitation of the relative density showed high levels of RAGE protein in the D-M group. The protein levels of RAGE were decreased in the D-M-A group (Figure 13A). In addition, western blot analysis showed that protein levels of TLR4 and TLR2 in ipsilateral hemisphere were increased in the D-M Group. However, the levels of TLR4 and TLR2 were markedly lowered after AGM treatment in the D-M-A group ($p < 0.05$, Figure 12 and 13B, C).

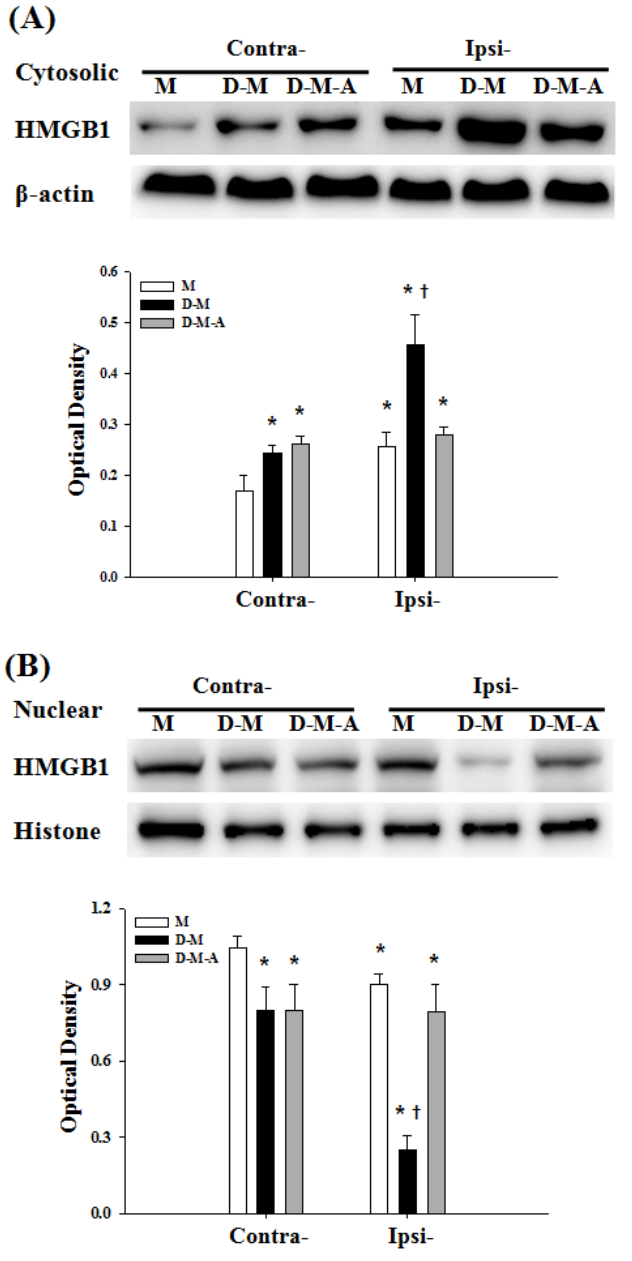

Figure 12. The protein levels of HMGB1 after treatment with AGM at 24 hours after reperfusion

(A and B) By using western blot analysis, HMGB1 protein levels in the

cytoplasm (A) and nucleus (B) were measured in all 3 groups. Nuclear HMGB1 was significantly reduced and cytosolic HMGB-1 was efficiently increased in the D-M group. The HMGB1 band (MW: 29 kDa) was detected in the ipsilateral hemisphere of the rat brain. The optical density of the bands was normalized to optical density bands for β-actin and histon. Data are presented as mean ± SEM (n = 5 per group). M: normoglycemic rats subjected to MCAO; D-M: diabetic rats subjected to MCAO; D-M-A: diabetic rats post-treated with AGM immediately after reperfusion. *$p < 0.05$ versus the M group, †$p < 0.05$ versus the D-M group.

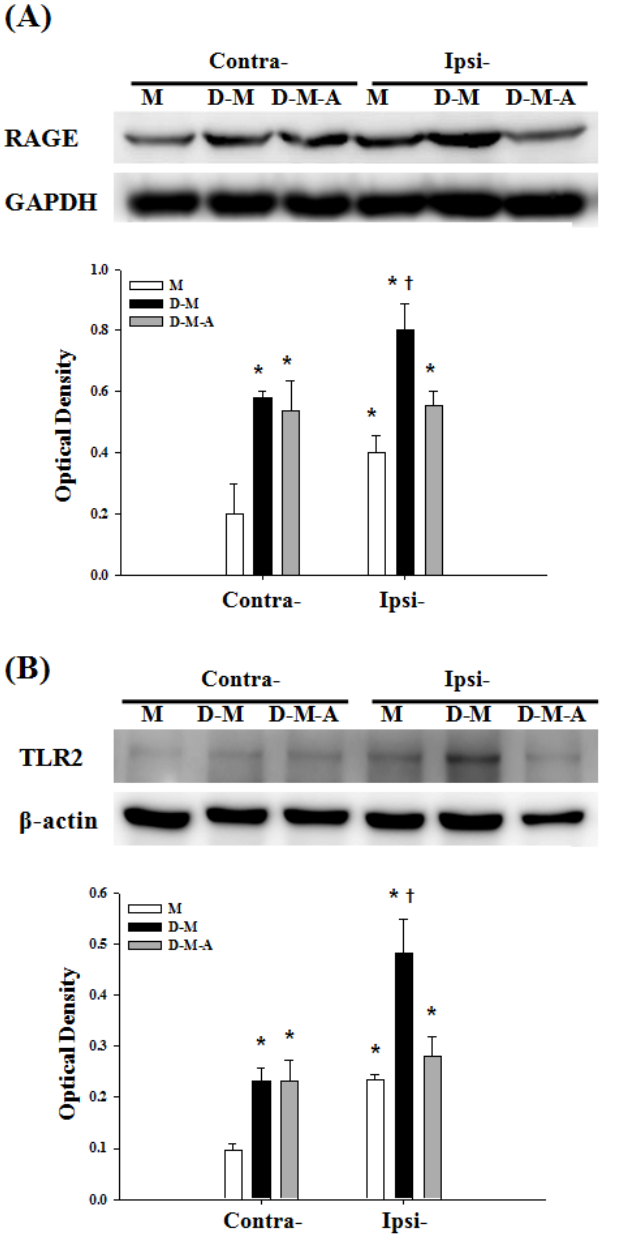
(A)
Contra-
Ipsi-
M
D-M
D-M-A
M
D-M
D-M-A
RAGE
GAPDH
Optical Density
M
D-M
D-M-A
Contra-
Ipsi-
(B)
Contra-
Ipsi-
M
D-M
D-M-A
M
D-M
D-M-A
TLR2
β-actin
Optical Density
M
D-M
D-M-A
Contra-
Ipsi-

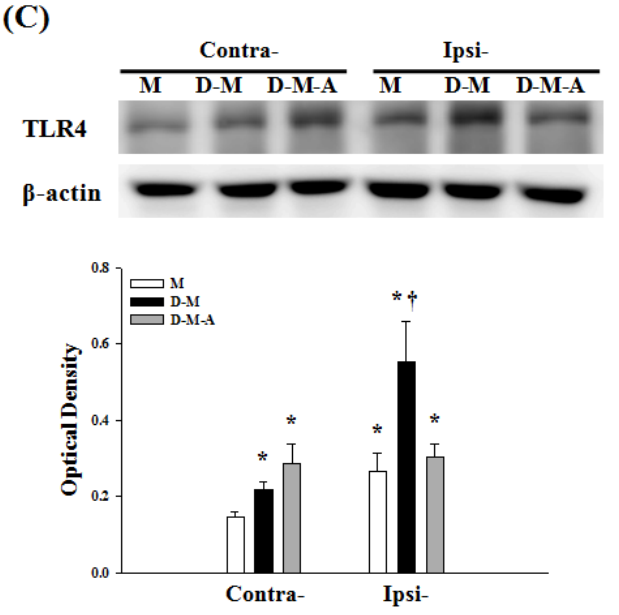

Figure 13. The levels of inflammation associated proteins, RAGE, TLR2, and TLR4 after treatment with AGM at 24 hours after reperfusion

(A) The relative optical density showed a reduced level of RAGE in the D-M-A group compared with D-M group (B and C) Protein levels of TLR2 and TLR4 were upregulated in the D-M group. However, after AGM treatment, TLR2 and TLR4 were decreased in the D-M-A group. The RAGE band (MW: 45 kDa), TLR2 band (MW: 90 kDa), and TLR4 (MW: 96 kDa) were detected in the ipsilateral hemisphere of the rat brain. The optical density of the bands was normalized to the optical density of β-actin and GAPDH bands. Data are presented as mean ± SEM (n = 5 per group). M: normoglycemic rats subjected to MCAO; D-M: diabetic rats subjected to MCAO; D-M-A: diabetic rats treated with AGM immediately after reperfusion. *$p < 0.05$ versus the M group, †$p < 0.05$ versus the D-M group.

AGM downregulated mRNA expression of HMGB1, RAGE, TLR2, and TLR4 at 24 hours after reperfusion

To investigate whether AGM could change mRNA expression of HMGB1, RAGE, TLR2, and TLR4, real-time PCR was performed to measure mRNA levels 24 hours after reperfusion. Assessment of HMGB1, RAGE, TLR2, and TLR4 mRNA in the ipsilateral hemisphere from the D-M group revealed a significant increase relative to the M and D-M-A groups. After AGM treatment, mRNA expression of HMGB1, RAGE, TLR2, and TLR4 were markedly attenuated in the ipsilateral hemisphere (Figure 14). These data were consistent with the results from the western blot analysis.

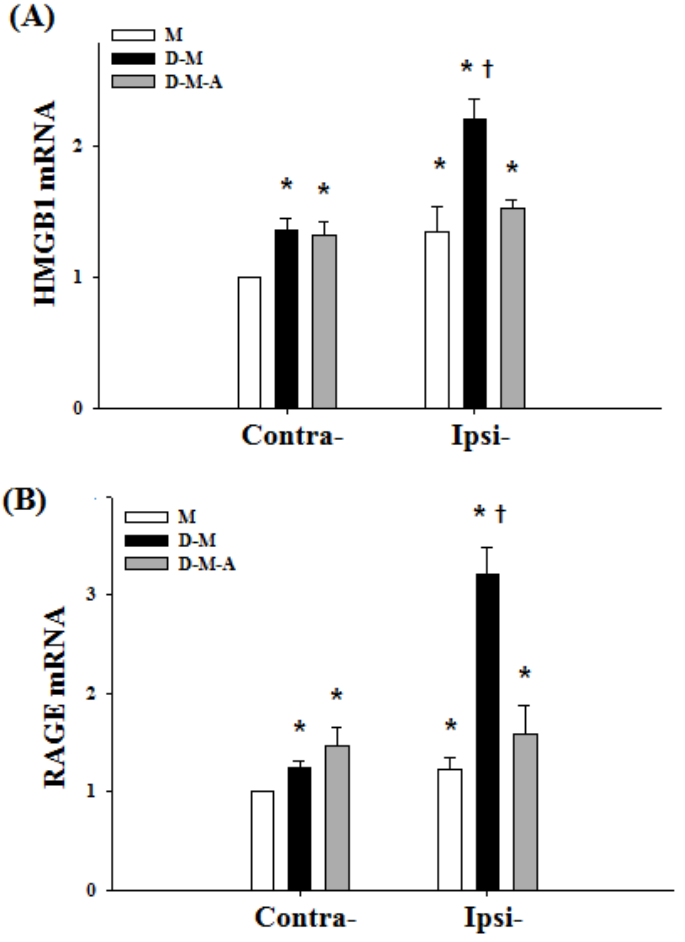

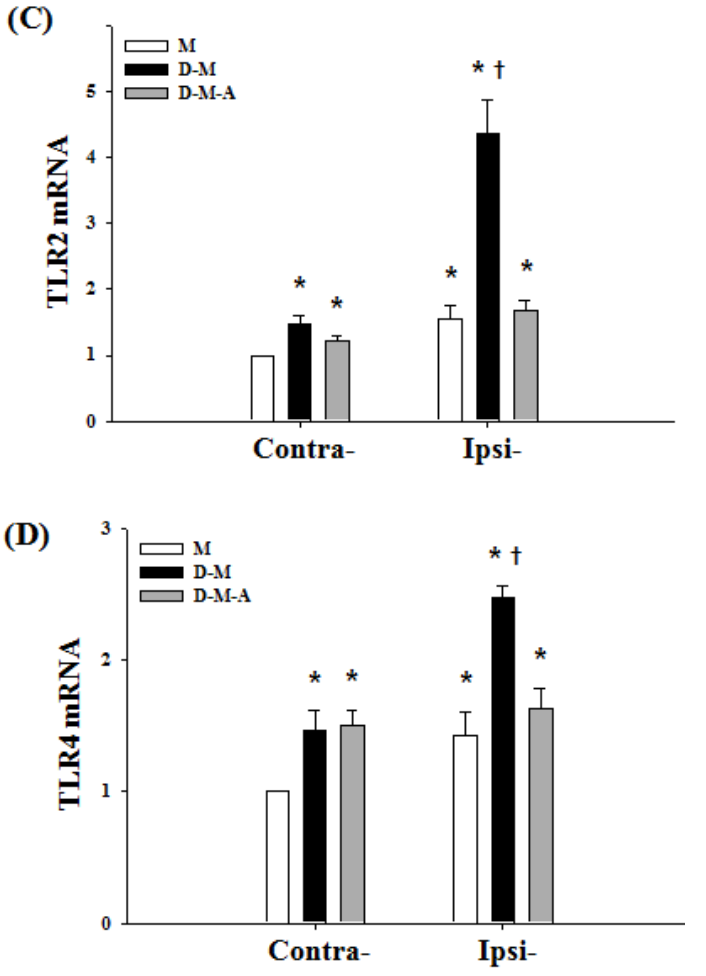

Figure 14. The mRNA expression of inflammation associated proteins, HMGB1, RAGE, TLR2, and TLR4 after treatment with AGM at 24 hours after reperfusion

The mRNA expression of HMGB1 (A), RAGE (B), TLR2 (C), and TLR4 (D), were measured by real-time PCR. In the ipsilateral hemisphere of the D-M group, HMGB1, RAGE, TLR2, and TLR4 mRNA expression was highly upregulated. However, levels of HMGB1, RAGE, TLR2, and TLR4 were lowered in the ipsilateral hemisphere of the D-M-A group compared with the D-M group. mRNA expression was calculated as the relative change in each

target gene normalized to β-actin. *$p < 0.05$ versus contralateral of M group. †$p < 0.01$ versus ipsilateral of M and D-M-A. There is no significance between the same symbol.

IV. DISCUSSION

The current study found that a single intraperitoneal injection of 100 $mg \cdot kg^{-1}$ AGM reduced the expression of inflammatory cytokines and their effects on brain injury after ischemia/reperfusion injury in diabetic rats. AGM reduced the increase of HMGB1, RAGE, TLR2, TLR4, NF-κB, IL-1β, and TNF-α. This suggests the possible neuroprotective effect of AGM in ischemia/reperfusion injury in diabetic rats is associated with suppressing neuroinflammation. Improved motor function and reduced infarct volume by AGM in diabetic rats could be due to reduced inflammation after ischemia/reperfusion.

Rizk *et al*[25] have reported that the brain infarct volume in diabetic rats after 2 hours of MCAO, followed by 24 hours of reperfusion, was approximately 10 times larger than in non-diabetic rats. In this study, the restoration of blood flow after 30 minutes of MCAO in non-diabetic rats produced a minimal infarct, but the infarct volume increased almost 4 to 6 times in STZ-induced diabetic rats under the same condition (Figure 2). Hyperglycemia itself is assumed to be a major factor responsible for excessive generation of reactive oxygen species (ROS). In DM, 'glucose toxicity' caused by augmentation of the intracellular glucose oxidation process and non-enzymatic glycation of protein molecules leads to overproduction of ROS.[26] In addition, the gene expression of IL-1β and IL-6 is much higher in type 2-diabetic mice with compared with normoglycemic mice.[6] Thus, enhanced oxidative stress and inflammatory responses induced by hyperglycemia may substantially contribute to the exacerbation of cerebral injury caused by transient ischemia and subsequent reperfusion in the diabetic state. The present findings seem to be consistent with other research stating the upregulated inflammatory cytokines in diabetes. The expression of inflammatory cytokines such as NF-κB, IL-1β, and TNF-α was increased in contralateral hemisphere of diabetic rats compared with normoglycemic rats ($p < 0.05$, Figure 6–11). In

addition, cytosolic HMGB1, RAGE, TLR2, and TLR4 were upregulated in the contralateral hemisphere of diabetic rats compared with normoglycemic rats ($p < 0.05$, Figure 13, 14). It is possible to hypothesize that such post-ischemic inflammation is likely to occur excessively in diabetes compared with normoglycemia, because baseline inflammation was upregulated in the diabetic rats. The current study has found that post-ischemic brain damage was more severe in the DM group compared with the normoglycemic control group.[4,27,28] These findings confirm the association between post-ischemic brain inflammation and brain injury in a diabetic model.

AGM is a putative neuromodulator in CNS neurons,[29,30] and is known to act as an agonist of imidazoline I and α_2-adrenergic receptors, an antagonist of N-Methyl-D-aspartic acid (NMDA) receptors, and an inhibitor of neuronal/inducible nitric oxide synthases (nNOS/iNOS).[29,30] Recently, AGM has received considerable attention due to its neuroprotective effects on ischemic neuronal injuries.[18,31,32] Most studies in the field of the neuroprotective effect of AGM have focused on the NOS pathway.[20,32-37] There has been little quantitative analysis of AGM's anti-inflammatory effect on post-ischemic neuronal damage. The most important clinically relevant finding in this study was that AGM post-treatment reduced post-ischemic neuronal inflammation in the diabetic rats subjected to MCAO. AGM decreased the expression of pro-inflammatory cytokines to less than half of the expression in DM rats subjected to 30 minutes of MCAO (Figure 6-11). The reduced infarct size was associated with a suppression of inflammatory changes in ischemia-reperfusion injury (Figure 3).

Inflammatory neurodegeneration is a crucial process contributing to cerebral damage after ischemia and reperfusion.[38] Inflammation is an integral part of the cascade of events triggered by ischemia and reperfusion.[12] HMGB1 is a ubiquitous and abundant nuclear protein; however, it is released from necrotic and inflammatory cells and induces an inflammatory cascade after

stimulation from a danger signal.[39] HMGB1 can function as an immune cytokine to enhance both innate and adaptive immune responses.[40] Recently, HMGB1 has received particular attention with respect to its pathological role in cerebral ischemia. In a rodent MCAO model, HMGB1 was found to be translocated from the nuclei into the cytoplasmic compartment at the early phase of ischemia.[41,42] High levels of serum HMGB1 are observed in stroke patients compared with healthy control subjects.[16] This early release of HMGB1 into the extracellular space after ischemic injury may contribute to the initial state of inflammatory response in the ischemic penumbra. It binds to receptor for advanced glycation end products (RAGE), toll-like receptor(TLR)2, and TLR4.[12] In the MCAO model, RAGE functions as a sensor for necrotic cell death and contributes to inflammation and ischemic brain damage.[16] TLR2 and TLR4 upregulate pro-inflammatory gene expression through the transcription factor NFκ-B and TNF-α.[43,44] NF-κB and TNF-α have been shown to play crucial roles in brain ischemia.[45-47] Activation of NF-κB leads to an increase in the expression of cyclooxygenase-2 (COX-2), iNOS, and pro-inflammatory cytokines, including TNFα, IL-1β, and IL-6, which accelerate inflammatory responses and promote neuronal cell death in the ischemic region.[38] Muhammad *et al*[16] have demonstrated that a neutralizing anti-HMGB1 antibody and an antagonist of HMGB1 at RAGE ameliorate ischemic brain damage in stroke patients. He has reported that the neutralizing anti-HMGB1 antibody, or the HMGB1 antagonist A box, may be used as specific tools to interfere with inflammation in stroke. In this study, AGM's effect of lowering the cytosolic translocation of HMGB1 reduced ischemic brain damage in diabetic rats with MCAO. These results match those observed in earlier studies.

To date, the neuroprotective effect of AGM on ischemia-reperfusion injury was known to be inhibitory to both nNOS and iNOS.[19,32] As mentioned previously, iNOS promotes neuronal cell death in the ischemic region and AGM is neuroprotective after ischemia-reperfusion injury by inhibiting iNOS.[20]

However, AGM interacts with many receptors, including the α-adrenergic, imidazoline, and NMDA receptors.[19,48] In this study, AGM was neuroprotective, *via* anti-inflammatory mechanisms, following ischemia-reperfusion injury in a diabetic rat model. AGM reduced the expression of HMGB1, RAGE, TLR2, and TLR4. In addition, AGM decreased the level of TNF-α, NF-κB, and IL-1β. The increased infarct size in the diabetic brain, compared with the normal brain after reperfusion, may be associated with already increased baseline inflammatory cytokines before the ischemic event. Therefore, further studies with greater focus on the anti-inflammatory effect of AGM in normoglycemic conditions are suggested.

AGM also lowers plasma glucose in a diabetic rat model. Hwang *et al* have reported that 60 $mg \cdot kg^{-1}$ AGM might enhance the secretion of β-endorphins, resulting in a lowering of plasma glucose in diabetic rats that lack insulin. Its maximal effect is reached at 30 minutes after AGM injection.[49] However, 24 hours after an intraperitoneal injection of 100 $mg \cdot kg^{-1}$ AGM, no difference in weight loss and glucose levels was found in this study. Considering that the glucose lowering effect of AGM lasts less than 6 hours after ischemia-reperfusion injury, the post conditioning single intraperitoneal injection of AGM has a novel neuroprotective effect distinct from its glucose controlling effect. In a similar context, AGM significantly conserved ^{18}FDG uptake in diabetic rats subjected to 30 minutes of MCAO (Figure 4). ^{18}FDG microPET imaging showed that the glucose metabolism in the ipsilateral hemisphere of diabetic rats was more impaired compared with the other groups and AGM produced a significant preservation of brain glucose metabolism after ischemia-reperfusion injury. Nathan *et al* have demonstrated that brain glucose metabolism, measured by microPET imaging, correlated well with cerebral blood flow determined by Laser doppler flowmetry in a 2 hour MCAO model.[50] Therefore, it can be suggested that AGM may attenuate the impairment of neuronal glucose metabolism by reducing infarct volume after

ischemia-reperfusion injury.

This study has successfully demonstrated that AGM reduces cytoplasmic translocation of HMGB1 and reduces neuronal injury after ischemia-reperfusion injury. Zhang *et al* have shown that HMGB1 translocation is both time and cell-type dependent.[51] The translocation of HMGB1 may be the result of chemical modification of HMGB1, such as *via* acetylation, phosphorylation, or methylation.[52-54] Previous studies have noted that cellular release of HMGB-1 was detected by immunoblot analysis of cerebrospinal fluid as early as 2 hour after ischemic reperfusion in 2 hour MCAO rat model.[42] Based on the results of this study, post-conditioning using a single bolus dose of AGM would reduce the initial inflammatory response, including HMGB1 release. This research has thrown up many questions in need of further investigation. It would be interesting to assess on the dose-response effect of AGM for diabetic rats. The AGM dose used in this study was based on previous studies of which were tested in normoglycemic rats; therefore, different doses may have resulted in a further decrease in infarct size and neurological deficit. In addition, the neurological deficit was investigated for only a short recovery period. Because neurological deficits can last years after the ischemic insult, more research is needed to elucidate the long-term effect of AGM.

V. CONCLUSION

In conclusion, AGM post-treatment immediately following 30 minutes of MCAO reduced infarct size and neurological deficit in diabetic rats. AGM effectively inhibited translocation of NF-κB and decreased the release of inflammatory cytokines after transient cerebral ischemia in diabetic rats, which might result from the down regulation of the innate immune response.

REFERENCES

1. Donnan GA, Fisher M, Macleod M, Davis SM. Stroke. Lancet 2008;371:1612-23.
2. Lopez AD, Mathers CD, Ezzati M, Jamison DT, Murray CJ. Global and regional burden of disease and risk factors, 2001: systematic analysis of population health data. Lancet 2006;367:1747-57.
3. Danaei G, Finucane MM, Lu Y, Singh GM, Cowan MJ, Paciorek CJ, et al. National, regional, and global trends in fasting plasma glucose and diabetes prevalence since 1980: systematic analysis of health examination surveys and epidemiological studies with 370 country-years and 2.7 million participants. Lancet 2011;378:31-40.
4. Luitse MJ, Biessels GJ, Rutten GE, Kappelle LJ. Diabetes, hyperglycaemia, and acute ischaemic stroke. Lancet Neurol 2012;11:261-71.
5. Sarwar N, Gao P, Seshasai SR, Gobin R, Kaptoge S, Di Angelantonio E, et al. Diabetes mellitus, fasting blood glucose concentration, and risk of vascular disease: a collaborative meta-analysis of 102 prospective studies. Lancet 2010;375:2215-22.
6. Tureyen K, Bowen K, Liang J, Dempsey RJ, Vemuganti R. Exacerbated brain damage, edema and inflammation in type-2 diabetic mice subjected to focal ischemia. J Neurochem 2011;116:499-507.
7. Sonnen JA, Larson EB, Brickell K, Crane PK, Woltjer R, Montine TJ, et al. Different patterns of cerebral injury in dementia with or without diabetes. Arch Neurol 2009;66:315-22.
8. Granic I, Dolga AM, Nijholt IM, van Dijk G, Eisel UL. Inflammation and NF-kappaB in Alzheimer's disease and diabetes. J Alzheimers Dis 2009;16:809-21.
9. Ibrahim S, Rashed L, Fadda S. Evaluation of renal gene expression of protein kinase C (PKC) isoforms in diabetic and nondiabetic

proliferative glomerular diseases. ScientificWorldJournal 2008;8:835-44.

10. Ramana KV, Tammali R, Reddy AB, Bhatnagar A, Srivastava SK. Aldose reductase-regulated tumor necrosis factor-alpha production is essential for high glucose-induced vascular smooth muscle cell growth. Endocrinology 2007;148:4371-84.
11. Ramasamy R, Vannucci SJ, Yan SS, Herold K, Yan SF, Schmidt AM. Advanced glycation end products and RAGE: a common thread in aging, diabetes, neurodegeneration, and inflammation. Glycobiology 2005;15:16r-28r.
12. Iadecola C, Anrather J. The immunology of stroke: from mechanisms to translation. Nat Med 2011;17:796-808.
13. Wang YC, Lin S, Yang QW. Toll-like receptors in cerebral ischemic inflammatory injury. J Neuroinflammation 2011;8:134.
14. Yang QW, Wang JZ, Li JC, Zhou Y, Zhong Q, Lu FL, et al. High-mobility group protein box-1 and its relevance to cerebral ischemia. J Cereb Blood Flow Metab 2010;30:243-54.
15. Goldstein RS, Gallowitsch-Puerta M, Yang L, Rosas-Ballina M, Huston JM, Czura CJ, et al. Elevated high-mobility group box 1 levels in patients with cerebral and myocardial ischemia. Shock 2006;25:571-4.
16. Muhammad S, Barakat W, Stoyanov S, Murikinati S, Yang H, Tracey KJ, et al. The HMGB1 receptor RAGE mediates ischemic brain damage. J Neurosci 2008;28:12023-31.
17. Li G, Regunathan S, Barrow CJ, Eshraghi J, Cooper R, Reis DJ. Agmatine: an endogenous clonidine-displacing substance in the brain. Science 1994;263:966-9.
18. Kim JH, Yenari MA, Giffard RG, Cho SW, Park KA, Lee JE. Agmatine reduces infarct area in a mouse model of transient focal cerebral ischemia and protects cultured neurons from ischemia-like

injury. Exp Neurol 2004;189:122-30.

19. Fairbanks CA, Schreiber KL, Brewer KL, Yu CG, Stone LS, Kitto KF, et al. Agmatine reverses pain induced by inflammation, neuropathy, and spinal cord injury. Proc Natl Acad Sci U S A 2000;97:10584-9.
20. Cui H, Lee JH, Kim JY, Koo BN, Lee JE. The neuroprotective effect of agmatine after focal cerebral ischemia in diabetic rats. J Neurosurg Anesthesiol 2012;24:39-50.
21. Garcia JH, Wagner S, Liu KF, Hu XJ. Neurological deficit and extent of neuronal necrosis attributable to middle cerebral artery occlusion in rats. Statistical validation. Stroke 1995;26:627-34; discussion 35.
22. Hunter AJ, Hatcher J, Virley D, Nelson P, Irving E, Hadingham SJ, et al. Functional assessments in mice and rats after focal stroke. Neuropharmacology 2000;39:806-16.
23. Kim JH, Lee YW, Park KA, Lee WT, Lee JE. Agmatine attenuates brain edema through reducing the expression of aquaporin-1 after cerebral ischemia. J Cereb Blood Flow Metab 2010;30:943-9.
24. Park JS, Arcaroli J, Yum HK, Yang H, Wang H, Yang KY, et al. Activation of gene expression in human neutrophils by high mobility group box 1 protein. Am J Physiol Cell Physiol 2003;284:C870-9.
25. Rizk NN, Rafols JA, Dunbar JC. Cerebral ischemia-induced apoptosis and necrosis in normal and diabetic rats: effects of insulin and C-peptide. Brain Res 2006;1096:204-12.
26. Baynes JW. Role of oxidative stress in development of complications in diabetes. Diabetes 1991;40:405-12.
27. Ott A, Stolk RP, van Harskamp F, Pols HA, Hofman A, Breteler MM. Diabetes mellitus and the risk of dementia: The Rotterdam Study. Neurology 1999;53:1937-42.
28. Arvanitakis Z, Wilson RS, Bienias JL, Evans DA, Bennett DA. Diabetes mellitus and risk of Alzheimer disease and decline in cognitive

function. Arch Neurol 2004;61:661-6.

29. Reis DJ, Regunathan S. Is agmatine a novel neurotransmitter in brain? Trends Pharmacol Sci 2000;21:187-93.

30. Halaris A, Plietz J. Agmatine : metabolic pathway and spectrum of activity in brain. CNS Drugs 2007;21:885-900.

31. Hong S, Lee JE, Kim CY, Seong GJ. Agmatine protects retinal ganglion cells from hypoxia-induced apoptosis in transformed rat retinal ganglion cell line. BMC Neurosci 2007;8:81.

32. Feng Y, Piletz JE, Leblanc MH. Agmatine suppresses nitric oxide production and attenuates hypoxic-ischemic brain injury in neonatal rats. Pediatr Res 2002;52:606-11.

33. Lortie MJ, Novotny WF, Peterson OW, Vallon V, Malvey K, Mendonca M, et al. Agmatine, a bioactive metabolite of arginine. Production, degradation, and functional effects in the kidney of the rat. J Clin Invest 1996;97:413-20.

34. Ahn SK, Hong S, Park YM, Lee WT, Park KA, Lee JE. Effects of agmatine on hypoxic microglia and activity of nitric oxide synthase. Brain Res 2011;1373:48-54.

35. Mun CH, Lee WT, Park KA, Lee JE. Regulation of endothelial nitric oxide synthase by agmatine after transient global cerebral ischemia in rat brain. Anat Cell Biol 2010;43:230-40.

36. Payandemehr B, Rahimian R, Bahremand A, Ebrahimi A, Saadat S, Moghaddas P, et al. Role of nitric oxide in additive anticonvulsant effects of agmatine and morphine. Physiol Behav 2013;118:52-7.

37. Satriano J, Cunard R, Peterson OW, Dousa T, Gabbai FB, Blantz RC. Effects on kidney filtration rate by agmatine requires activation of ryanodine channels for nitric oxide generation. Am J Physiol Renal Physiol 2008;294:F795-800.

38. Brown GC, Neher JJ. Inflammatory neurodegeneration and mechanisms

of microglial killing of neurons. Mol Neurobiol 2010;41:242-7.

39. Lotze MT, Tracey KJ. High-mobility group box 1 protein (HMGB1): nuclear weapon in the immune arsenal. Nat Rev Immunol 2005;5:331-42.

40. Ulloa L, Messmer D. High-mobility group box 1 (HMGB1) protein: friend and foe. Cytokine Growth Factor Rev 2006;17:189-201.

41. Kim JB, Sig Choi J, Yu YM, Nam K, Piao CS, Kim SW, et al. HMGB1, a novel cytokine-like mediator linking acute neuronal death and delayed neuroinflammation in the postischemic brain. J Neurosci 2006;26:6413-21.

42. Qiu J, Nishimura M, Wang Y, Sims JR, Qiu S, Savitz SI, et al. Early release of HMGB-1 from neurons after the onset of brain ischemia. J Cereb Blood Flow Metab 2008;28:927-38.

43. Broad A, Kirby JA, Jones DE. Toll-like receptor interactions: tolerance of MyD88-dependent cytokines but enhancement of MyD88-independent interferon-beta production. Immunology 2007;120:103-11.

44. Marsh BJ, Williams-Karnesky RL, Stenzel-Poore MP. Toll-like receptor signaling in endogenous neuroprotection and stroke. Neuroscience 2009;158:1007-20.

45. Hosomi N, Ban CR, Naya T, Takahashi T, Guo P, Song XY, et al. Tumor necrosis factor-alpha neutralization reduced cerebral edema through inhibition of matrix metalloproteinase production after transient focal cerebral ischemia. J Cereb Blood Flow Metab 2005;25:959-67.

46. Ridder DA, Schwaninger M. NF-kappaB signaling in cerebral ischemia. Neuroscience 2009;158:995-1006.

47. Rosenzweig HL, Minami M, Lessov NS, Coste SC, Stevens SL, Henshall DC, et al. Endotoxin preconditioning protects against the cytotoxic effects of TNFalpha after stroke: a novel role for TNFalpha in

LPS-ischemic tolerance. J Cereb Blood Flow Metab 2007;27:1663-74.

48. Horvath G, Kekesi G, Dobos I, Szikszay M, Klimscha W, Benedek G. Effect of intrathecal agmatine on inflammation-induced thermal hyperalgesia in rats. Eur J Pharmacol 1999;368:197-204.

49. Hwang SL, Liu IM, Tzeng TF, Cheng JT. Activation of imidazoline receptors in adrenal gland to lower plasma glucose in streptozotocin-induced diabetic rats. Diabetologia 2005;48:767-75.

50. Zwagerman N, Sprague S, Davis MD, Daniels B, Goel G, Ding Y. Pre-ischemic exercise preserves cerebral blood flow during reperfusion in stroke. Neurol Res 2010;32:523-9.

51. Zhang J, Takahashi HK, Liu K, Wake H, Liu R, Maruo T, et al. Anti-high mobility group box-1 monoclonal antibody protects the blood-brain barrier from ischemia-induced disruption in rats. Stroke 2011;42:1420-8.

52. Zhang Q, Wang Y. HMG modifications and nuclear function. Biochim Biophys Acta 2010;1799:28-36.

53. Youn JH, Shin JS. Nucleocytoplasmic shuttling of HMGB1 is regulated by phosphorylation that redirects it toward secretion. J Immunol 2006;177:7889-97.

54. Bonaldi T, Talamo F, Scaffidi P, Ferrera D, Porto A, Bachi A, et al. Monocytic cells hyperacetylate chromatin protein HMGB1 to redirect it towards secretion. EMBO J 2003;22:5551-60.

< ABSTRACT (IN KOREAN)>

당뇨와 병발된 뇌 허혈 쥐 모델에서 아그마틴의 항 염증 효과

<지도교수 구본녀>

연세대학교 대학원 의학과

김 정 민

배경: 당뇨는 중추신경계를 포함하여 여러 장기에 구조적 기능적인 이상을 유발시키는 대사성 질환이다. 당뇨는 정상 혈당군에 비해서 기저 염증 반응이 증가되어 있는데, 따라서 뇌 허혈 시 발생하는 염증반응이 당뇨군에서 증폭되어 나타나서 당뇨군에서 뇌허혈시 뇌손상 정도가 크다고 밝혀져 있다. 아그마틴은 뇌허혈 시 뇌보호 기능이 있음이 알려져 있으나, 그 정확한 기전에 대해서는 알려진 바가 적다. 본 연구의 목적은 당뇨 쥐 뇌허혈 후 재관류 모델에서 아그마틴의 뇌보호 효과에 대한 기전을 항염증 반응에 초점을 두고 밝혀 보고자 하였다.

방법: 정상혈당군 (30 마리)와 당뇨 유도군 (82 마리)을 대상으로 30분간 일시적으로 중뇌동맥 폐쇄하여 일시적 뇌허혈 모델을 만들고 재관류하였다. 당뇨군 중 일부에게(30마리) 아그마틴(100 mg/kg)을 재관류와 동시에 복강내 주사하였다. 뇌경색 재관류 후 운동능을 평가하기 위해서 신경학적 검사와 회전봉 테스트를 시행하였다. 뇌경색 크기를 TTC 염색과 micro-PET을 이용해서 비교하였다. Western blot과 면역조직학 검사를 통해서 허혈 뇌조직의 염증성 사이토카인을 측정하였다. Real-time PCR을 통해서 HMGB1, RAGE,

TLR2와 TLR4를 정량적으로 분석하였다.
결과: 아그마틴 치료군이 재관류 후 24시간, 72시간 후 신경행동학적 검사소견이 대조군에 비해서 호전되었고, 뇌경색 크기도 감소하였다. ($p < 0.05$) 면역조직학 검사결과에서 아그마틴 치료군이 재관류 24시간 72시간 후 염증성 사이토카인 분비가 감소하였다. Western blot과 RT-PCR 결과에서도 아그마틴군이 재관류 24시간에 선천성 면역의 사이토카인인 HMGB1, RAGE, TLR2, TLR4 의 발현을 감소하였다.($p < 0.05$)
결론: 당뇨 쥐에서 30분 중뇌동맥 결찰로 유도한 일시적 뇌허혈 재관류 모델에서 재관류 직 후 복강내 주입한 아그마틴 치료가 뇌경색크기를 줄이고 신경학적 뇌 손상 정도를 감소시켰다. 이러한 아그마틴의 뇌보호효과는 경색 후 뇌의 단계적 염증 반응을 조율하는데 연관되어 있을 것으로 사료된다.

핵심 되는 말: 아그마틴, 당뇨, 염증, 선천면역, 허혈 후 재관류 손상